



Switchable adhesive films of pullulan loaded with a deep eutectic solvent-curcumin formulation for the photodynamic treatment of drug-resistant skin infections

Sónia N. Pedro^a, Bruno F.A. Valente^a, Carla Vilela^a, Helena Oliveira^b, Adelaide Almeida^b, Mara G. Freire^a, Armando J.D. Silvestre^a, Carmen S.R. Freire^{a,*}

^a CICECO - Aveiro Institute of Materials, Department of Chemistry, University of Aveiro, Campus de Santiago, 3810-193, Aveiro, Portugal

^b CESAM, Department of Biology, University of Aveiro, Campus de Santiago, 3810-193, Aveiro, Portugal

ARTICLE INFO

Keywords:

Adhesive films
Bacterial resistance
Pullulan
Curcumin
Deep eutectic solvents
Photodynamic therapy
Skin infections
Switchable behavior

ABSTRACT

Antimicrobial photodynamic therapy (aPDT) is a potent tool to surpass the global rise of antimicrobial resistance; still, the effective topical administration of photosensitizers remains a challenge. Biopolymer-based adhesive films can safely extend the residence time of photosensitizers. However, their wide application is narrowed by their limited water absorption capacity and gel strength. In this study, pullulan-based films with a switchable character (from a solid film to an adhesive hydrogel) were developed. This was accomplished by the incorporation of a betaine-based deep eutectic solvent (DES) containing curcumin ($4.4 \mu\text{g}\cdot\text{cm}^{-2}$) into the pullulan films, which tuned the films' skin moisture absorption ability, and therefore they switch into an adhesive hydrogel capable of delivering the photosensitizer. The obtained transparent films presented higher extensibility (elongation at break up to 338.2%) than the pullulan counterparts (6.08%), when stored at 54% of relative humidity, and the corresponding hydrogels a 4-fold higher adhesiveness than commercial hydrogels. These non-cytotoxic adhesives allowed the inactivation (~ 5 log reduction), down to the detection limit of the method, of multi-resistant strains of *Staphylococcus aureus* in *ex vivo* skin samples. Overall, these materials are promising for aPDT in the treatment of resistant skin infections, while being easily removed from the skin.

1. Introduction

Antimicrobial resistance has challenged the global healthcare system, becoming a threat during recent decades to treat antibiotic-resistant infections [1,2]. Particularly, the migration of methicillin-resistant *Staphylococcus aureus* (MRSA) from its hospital confinement and long-term care facilities to community-acquired infections has narrowed the number of antibiotics that are still effective to tackle this critical health problem [3]. In the search for alternative strategies to treat multidrug-resistant skin infections, antimicrobial photodynamic therapy (aPDT) has proven to be a promising option [4]. This approach uses light with appropriate wavelengths, along with a photosensitizing agent, which in the presence of molecular oxygen generates oxidant species [reactive oxygen species (ROS) like superoxide and singlet oxygen, ($^1\text{O}_2$)], that kill pathogens, including multidrug resistant bacteria [5].

Several aPDT approaches and photosensitizers have been studied in

an attempt to inactivate MRSA infections, including the exploitation of biopolymeric drug delivery systems to improve the therapeutic efficacy of photosensitizer agents [6]. Curcumin is, an example of a natural and low cytotoxic photosensitizer, that has gained increased relevance due to its photodynamic activity, as well as anti-inflammatory and antimicrobial actions [6,7]. Nevertheless, its poor aqueous solubility and low aqueous photostability hinders its application in aPDT but also its inclusion in biopolymeric drug delivery systems. To this purpose, the development of curcumin formulations with improved water solubility and of adequate biopolymeric delivery systems capable to release the photosensitizer at the infection site, while being transparent for light activating purposes, remains a challenging task.

Within biopolymeric drug delivery systems, hydrogels have been recently considered in aPDT treatments for wound therapy [8]. The advantage of these systems is the dual capacity for being used as both bandage material and delivery system, while providing a moist healing environment [9,10]. Hydrogels originated from natural polymers, such

* Corresponding author.

E-mail address: cfreire@ua.pt (C.S.R. Freire).

<https://doi.org/10.1016/j.mtbio.2023.100733>

Received 6 February 2023; Received in revised form 30 June 2023; Accepted 12 July 2023

Available online 14 July 2023

2590-0064/© 2023 The Authors. Published by Elsevier Ltd. This is an open access article under the CC BY-NC-ND license (<http://creativecommons.org/licenses/by-nc-nd/4.0/>).

as alginate [11], keratin [11] and chitosan [12,13], have been applied for aPDT purposes. Adhesive hydrogel films have the advantage of extending the residence time, allowing to prolong the local therapeutic action [14]. These delivery systems are usually designed as flexible systems that can easily adapt to the site of application, being more comfortable to use from the patient's perspective [15,16]. Biopolymers like silk [17] and chitosan [12,13] have been applied in the production of adhesives aiming to be applied in aPDT for tissue repair and oral and skin application purposes. The use of natural polymers in this area has shown to enhance cell proliferation and tissue differentiation, allowing to inhibit wound infection while promoting wound repair, which would be desirable in the treatment of skin infections [18,19]. Yet, some of these biopolymers still display low water absorption capacity and gel strength, which need to be ideally targeted to develop appropriate biopolymer-based systems for aPDT therapy [20,21].

Pullulan is an example of a polysaccharide that originates highly transparent materials such as films [22], which is an appealing feature for application as supports on aPDT. Additionally, this polysaccharide possesses good mechanical performance, thermal stability and excellent water solubility [23,24]. Pullulan has also been reported for its ability to improve wounds re-epithelialization, dermal regeneration, blood vessels formation and collagen synthesis, proving that pullulan gels could be potential wound healing agents [25]. However, so far, the application of pullulan-based systems in this domain is limited and is mostly focused on mucoadhesive-based systems for oral administration [26], and to a smaller extent, to produce nanoparticles and nanogels for the photodynamic therapy of cancer [27,28].

Finally, improving the solubility of photosensitizers in aqueous media while being compatible with hydrophilic biopolymers like pullulan can be tackled in distinct ways [29,30], among which deep eutectic solvent (DES) aqueous solutions have attracted significant attention. DES can be described as a mixture of two compounds (a hydrogen bond acceptor (HBA) and a hydrogen bond donor (HBD)) that have a decreased melting point when compared to the individual components, becoming liquid at room or body temperature. DES can be formulated based on a myriad of HBDs (e.g. carboxylic acids), and HBAs (e.g. ammonium salts), among which the use of nontoxic natural compounds is extremely attractive by their inherent biocompatibility [31, 32]. Among the vast panoply of interesting properties, the potential of adequately selected DES, and their aqueous solutions, to improve solubility and bioactivity of hydrophobic active ingredients, is of particular relevance in the context of the present study, as recently demonstrated [33,34].

Herein, we aimed to develop a biopolymer-based adhesive film loaded with a photosensitizer that could present enhanced mechanical and adhesive properties, as well as superior photodynamic action, for topical application. To this purpose, the application of pullulan and curcumin, in the development of a delivery system to be used as aPDT towards skin infections is explored. Furthermore, this system presents a switchable character when in contact with skin moisture by transitioning from a solid film into a highly adhesive hydrogel, achieved by the incorporation of an aqueous solution of a deep eutectic solvent (DES) composed of betaine (skin humectant with osmoprotectant properties [35]) and levulinic acid (commonly used in skincare products). Due to their versatility of design, DES can be fine-tuned to a specific formulation purpose and to present low cytotoxicity. Therefore, this betaine-based DES can be considered a non-cytotoxic and environmentally friendly solvent, which was used to prepare curcumin formulations with improved water solubility that were incorporated into the pullulan-based films. The resultant pullulan-based films can simultaneously adhere to skin, switch into a hydrogel and deliver the photosensitizer in an infected area, and thus enhance the photodynamic action of curcumin. All films were characterized in terms of optical, thermal and mechanical properties, and the adhesiveness of the final films was tested on *ex-vivo* skin samples. The photodynamic antimicrobial action was initially studied in *S. aureus* ATCC 6538 in solution and then, as a

proof-of-concept, was tested against MRSA strains on *ex-vivo* skin samples.

2. Materials and methods

2.1. Chemicals and cell culturing

The DES studied herein was prepared by combining betaine anhydrous (98%, Alfa Aesar, Germany) and levulinic acid ($\geq 98\%$, Sigma-Aldrich, St. Louis, Missouri, USA). The photosensitizer used was curcumin (≥ 95 , Sigma-Aldrich, St. Louis, Missouri, USA). Pullulan powder (98%, MW 272 kDa) was supplied by B&K Technology Group (Xiamen, China). MTT (3-(4,5-dimethylthiazol-2-yl)-2,5-diphenyltetrazolium-bromide) was purchased from Sigma-Aldrich (St. Louis, Missouri, USA). Other reagents and solvents were from analytical or high-performance liquid chromatography (HPLC) grades. For the bacterial cultures, Tryptic Soy Broth medium (TSB) and Tryptic Soy Agar (TSA) were used and supplied by Liofilchem (TE, Italy). The phosphate buffered saline solution (PBS, pH 7.4) was prepared by dissolution of tablets acquired from Sigma-Aldrich (St. Louis, Missouri, USA). Immortalized human epidermal keratinocytes (HaCaT cells) obtained from Cell Lines Services (Eppelheim, Germany) were cultured in Dulbecco's modified Eagle's medium (DMEM) supplemented with 10% of fetal bovine serum (FBS) and 1% of L-glutamine, penicillin–streptomycin and fungizone (Life Technologies, Grand Island, NY, USA) and incubated with 5% CO₂ in a humidified atmosphere at 37 °C.

2.2. DES preparation

The DES investigated in this work was prepared by the heating method by mixing the respective precursors (betaine and levulinic acid, Bet:Lev) in sealed glass vials at 1:1 molar ratio, instead of the typical 1:2 [36], to minimize the acid content. These vials were placed under constant heating and stirring until a homogeneous transparent liquid was obtained (maximum temperature of 85 °C). The DES was then allowed to return to room temperature. The respective DES components' integrity was confirmed by ¹H NMR and ¹³C NMR spectroscopy. The referred spectra were recorded using a Bruker Avance 300 at 300.13 MHz and 75.47 MHz, respectively, in deuterated water and using trimethylsilylpropanoic acid (TMS) as an internal reference.

2.3. Curcumin's solubility assay

The determination of the solubility of curcumin in water and in the aqueous solutions of Bet:Lev followed a previously reported procedure [33]. Briefly, the solubility was determined by saturation of 2.0 g of pure water or of each DES aqueous solution (0–90% (w/w) of DES) with curcumin at both room (25 °C) and human body (37 °C) temperatures. A measured aliquot of each saturated solution was diluted to a well-defined final total v/v, carefully filtered with a 0.45 μm syringe filter to remove any solid and subsequently quantified by high-performance liquid chromatography with diode-array detection (HPLC-DAD) (Shimadzu, model PROMINENCE, Kyoto, Japan) to determine the curcumin solubility. HPLC analyses were performed with an analytical C18 reversed-phase column (250 × 4.60 mm²), Kinetex 5 μm C18 100 Å, from Phenomenex conducted in isocratic mode under a flow rate of 1 mL min⁻¹ and operated at 35 °C. The mobile phase contained 40% (v/v) of methanol, 15% (v/v) of acetonitrile and 45% (v/v) of ultra-pure water with 0.3% (v/v) of ortho-phosphoric acid. Samples were analyzed at 377 nm in duplicates and using an injection volume of 10 μL.

2.4. Photostability of curcumin in the Bet:Lev solution

Photostability was evaluated by placing the samples in 6-well plates filled with a final volume of 5 mL of PBS and under stirring. DES aqueous

solutions (50% w/w) comprising curcumin and aqueous solutions of curcumin solubilized in acetone (50% w/w) were added to each well to obtain specific curcumin concentrations in the range of 5–200 μM . After 15 min of incubation in the dark, the samples were exposed to a light source with an irradiance of 50 $\text{mW}\cdot\text{cm}^{-2}$ for 60 min. Aliquots (100 μL) of each well were collected at each 15 min and curcumin was quantified by HPLC-DAD using the previously described method. Three independent studies for each curcumin concentration were conducted, and each sample was analyzed at least in duplicate.

2.5. Preparation of the pullulan-based films

Four different pullulan-based films were prepared using an aqueous solution of 6.0% (w/v) of pullulan, i.e., films without the photosensitizer (PL), with curcumin solubilized in aqueous solution with acetone (PL-C) (4.4 $\mu\text{g}\cdot\text{cm}^{-2}$ dose), with the Bet:Lev aqueous solution (PL-DES) and with curcumin solution in aqueous Bet:Lev (PL-(DES + C) (4.4 $\mu\text{g}\cdot\text{cm}^{-2}$ dose). For the films with curcumin in aqueous Bet:Lev solution and the ones only with Bet:Lev aqueous solution, the DES was added to present the same concentration of the biopolymer (1:1 mass ratio). For the PL-C films, due to the low solubility of curcumin in water, the DES amount was replaced by aqueous acetone (both 50% w/w). Finally, films were obtained by casting the solutions in silicone plates with dimensions of 5 \times 15 cm^2 , placed at 40 $^{\circ}\text{C}$ in a ventilated oven overnight. All films were produced in triplicates. After preparation, the films were immediately used for each assay. Exceptionally, a set of films was stored for 24 h under a relative humidity (RH) of 54% (using a saturated solution of magnesium nitrate [37]) and at room temperature before being used for the mechanical assays.

2.6. UV-Vis spectroscopy

Transmittance spectra of the films were recorded at room temperature (200–800 nm). Acquisition was made with a Shimadzu UV-1800 UV-Vis spectrophotometer (Shimadzu Corp., Kyoto, Japan) equipped with a quartz window plate, bearing the holder in the vertical position. For better comprehension of the UV-Vis spectra in transmittance mode behavior of the films comprising the photosensitizer, curcumin absorption spectrum was also recorded in the same conditions.

2.7. FTIR-ATR spectroscopy

FTIR-ATR spectra were collected for all pullulan-based films and for the Bet:Lev and for the curcumin used (for comparison purposes). With this aim, a FTIR system Spectrum BX (Perkin-Elmer Inc., Waltham, Massachusetts, USA) equipped with a diamond crystal and a single horizontal Golden Gate ATR cell was used. All analyses were performed at room temperature with controlled relative humidity (75–80%) in the range of 4000–400 cm^{-1} with a resolution of 4 cm^{-1} and by accumulating 64 scans with an interval of 1 cm^{-1} . A background air spectrum was subtracted in all the spectra acquired, and the results were recorded as transmittance values.

2.8. Thermogravimetric analysis

Samples were heated at a constant rate of 10 $^{\circ}\text{C}\cdot\text{min}^{-1}$ from room temperature up to 800 $^{\circ}\text{C}$ under a nitrogen flow of 20 $\text{mL}\cdot\text{min}^{-1}$. The assays were carried out with a SETSYS Setaram TGA analyzer (SETARAM Instrumentation, France) equipped with a platinum cell.

2.9. Moisture uptake capacity

The moisture uptake measurement was conducted at two different relative humidity conditions, viz. 54 and 98% relative humidity. For that, film samples (PL, PL-C, PL-DES and PL-(DES + C)) were cut into squares (1 \times 1 cm^2), weighted, and placed in chamber desiccator

cabinets containing a saturated aqueous solution of magnesium nitrate (for 54% RH) or of potassium sulfate (for 98% of RH) [37]. Samples were weighted at specific time points during 48 h. The moisture uptake values of each film were calculated following Eq.

$$\text{Moisture uptake (\%)} = \left(\frac{w_t - w_0}{w_0} \right) \quad (1)$$

Where w_t and w_0 are the weight of the film after each time point of exposure to relative humidity (54 or 98%) and the initial weight of the films, respectively.

2.10. Mechanical tests

The mechanical properties of the pullulan-based films were evaluated through tensile tests performed on an Instron 5966 Series machine (Instron Corporation, Norwood, Massachusetts, USA). Analyses of the dried films were conducted in traction mode at a crosshead velocity of 10 $\text{mm}\cdot\text{min}^{-1}$ and using a static load cell of 500 N and at room temperature. Rectangular specimens (5 \times 1 cm^2) were used, and at least 5 replicates were tested for each sample, with final values expressed as the average \pm SD. The Young's modulus, the tensile stress and the elongation at break were calculated using the Bluehill 3 material testing software. Multiple group comparisons were executed by One-Way ANOVA analysis using GraphPad Prism, version 6.01 (GraphPad Software, San Diego, California, USA).

The mechanical properties of films stored at 54% of RH (close to skin conditions) were assessed at a crosshead velocity of 50 $\text{mm}\cdot\text{min}^{-1}$ and using a static load cell of 50 N, at room temperature.

2.11. Adhesive properties

Tissue adhesiveness was determined by following the 180-degree peel and lap-shear standard protocols with slight modifications (ASTM F2256 and ASTM F2255 respectively). Briefly, fresh porcine skin pieces obtained from a local butcher (7 \times 2.5 cm^2) were washed with PBS to clean the skin surface. Glass films, with 1 mm of thickness were applied using ethyl cyanoacrylate super glue (Loctite®) as a stiff backing for the skin pieces. Unless otherwise indicated, all adhesives were tested upon an adhesion area of 2.5 cm width and 2.5 cm length and adhere to the skin samples under gentle pressing; mechanical tests were performed 3 min after initial pressing to ensure moisturizing equilibrium of the adhered samples. The commercial adhesive tested (Hydrocoll®) was applied to the skin following the conditions provided in the manufacturer's manual. Since these do not possess double adhesive properties, they were unable to be used in lap-shear tests. All tests were performed in an Instron 5966 Series (Instron Corporation, Norwood, Massachusetts, USA) testing machine, equipped with a load cell of 50 kN and conducted with a constant speed of 10 $\text{mm}\cdot\text{min}^{-1}$. Interfacial toughness was calculated by measuring the peeling force until a plateau was achieved and then determined by dividing two times the resulting force by the width of the tested sample. Shear strength resulted from the ratio of the maximum force by the adhesion area (0.25 mm^2). Maximum adhesion force was distinguished as the point at which the two skin pieces started to detach.

2.12. Cell viability

Cell culturing followed the protocol previously reported [33]. The cytotoxic effect of the Bet:Lev formulations without the curcumin (20–50% (w/w) of DES), the curcumin formulated in Bet:Lev aqueous solutions (in a range of 0–25 μM of curcumin), and the pullulan film containing the Bet:Lev aqueous solution comprising curcumin (20 μM) was evaluated. HaCaT cells were seeded in 96-well plates at a concentration of 5000 $\text{cells}\cdot\text{mL}^{-1}$ and allowed to adhere for 24 h. After adhesion, cells were exposed to each formulation diluted in DMEM medium

and incubated for 24 h at 37 °C in 5% of CO₂. After this period, the wells were washed with PBS, and the cell viability was evaluated by the colorimetric MTT assay (1 mg.mL⁻¹ in PBS, pH 7.2), according to a previously reported protocol [33]. The percentage of viable cells was calculated as the ratio between the absorbance of treated versus the control cells (Ct).

2.13. Bacterial strains and culture conditions

Staphylococcus aureus ATCC 6538, *S. aureus* DSM 25693, a methicillin-resistant (MRSA) strain, positive for SE A, C, H, G, and I [38]; and MRSA M98070 strain isolated from a hospitalized patient at Hospital de Coimbra (Portugal), possessing the *mecA* gene, were used in this work. These strains were grown on Tryptic Soy Agar (TSA) medium at 37 °C for 24 h and posteriorly maintained at 4 °C. Each bacterium strain was inoculated whenever necessary in liquid medium Tryptic Soy Broth (TSB) and grown aerobically under stirring (100 rpm) at 37 °C for 24 h. Prior to each aPDT assay, an aliquot of this culture (300 µL) was transferred twice into a new fresh TSB medium (subcultured in 30 mL) and grew overnight at 37 °C also under stirring.

2.14. In vitro photodynamic assays

The photodynamic treatment was first tested *in vitro* against *S. aureus* ATCC 6538 to validate the system efficacy. The assays were performed in PBS in 6-well plates with a final volume of bacterial suspension of 5.0 mL per sample with a final bacterial concentration of ~10⁷ colony-forming unit per milliliter (CFU.mL⁻¹). Curcumin solutions in aqueous DES (50% w/w) and in aqueous solutions of acetone (50% w/w) were added to each well to attain a final concentration of 20 µM of curcumin. A blank of DES aqueous solution (50% w/w) (without the photosensitizer) was also tested for comparison purposes. Light and dark controls were also conducted along with the samples: in the light controls, a bacterial suspension in PBS was exposed to light without addition of photosensitizer solution in aqueous DES; for the dark controls, all samples were exposed to the same conditions (time points, stirring rate and temperature), however, protected from any light source. After the addition of the solutions to the bacterial suspension, and as previously mentioned, the final solutions were incubated in the dark for 15 min under stirring to promote the binding of the photosensitizer to the bacterial cells. After dark incubation, the samples and light controls were exposed to a white light-emitting diode (LED) at an irradiance of 50 mW.cm⁻², for 90 min under stirring. Dark controls were analyzed over the same period. Aliquots (100 µL) of each sample and of each control were collected at specific time points (0, 15, 30, 45 and 60 min). These were serially diluted in PBS and pour-plated in TSA Petri dishes. After incorporation of the photosensitizer on pullulan-based films, we also tested *in vitro* the efficacy of the PL, PL-C, PL-DES and PL-(DES + C) films (2.5 × 2.5 cm²) solubilized in the *S. aureus* suspension (5.0 mL) following the previously described aPDT protocol but extending the irradiation time to 90 min. Experiments were carried out in triplicated and repeated three times for each condition.

2.15. Analysis of singlet oxygen and free radicals scavengers production

The responsible mechanism for curcumin's activity in the PL-(DES + C) films, was evaluated by addition of appropriated amounts of two different scavengers, namely D-mannitol (to detect free radicals, type I mechanism) and L-histidine (to detect singlet oxygen, type II mechanism) to a bacterial suspension of *S. aureus* ATCC 6538 (for a final concentration of 100 mM) [39], using the same experimental conditions of the *in vitro* photodynamic assays. Then, pullulan with Bet:Lev and curcumin at 20 µM were added to the suspension. The final suspensions were incubated in the dark for 15 min, and then irradiated as previously described, for 90 min under stirring. Once again, aliquots (100 µL) of each sample and of each control were collected at specific time points (0,

15, 30, 60 and 90 min), serially diluted in PBS and pour-plated in TSA Petri dishes. During the assay solutions were kept at room temperature and under stirring. Experiments were carried out in triplicated and repeated three times for each condition.

2.16. Photoinactivation on skin (ex vivo assay)

After the *in vitro* assays, we studied the inactivation of the collection strain of *S. aureus* and both MRSA strains in *ex vivo* models after application of novel pullulan-based films. Porcine skin samples were prepared by cleaning with cold running water and the remaining water was dried using soft filter paper. After dried, the adipose tissue was removed using a scalpel. The skin was cut under sterile conditions into 9 cm² pieces (3 × 3 cm²) and placed in sterilized 6-well plates. The skin samples were sprayed with 70% ethanol, incubated for 15 min, and then placed under ultraviolet radiation, for 30 min each side. After the removal of the resident bacteria, the skin samples were subjected to bacterial contamination with *S. aureus* or MRSA strains. Each strain was grown overnight and diluted in PBS to be equally distributed over the skin, in order to obtain a concentration of ~10⁷ CFU.mL⁻¹. After 1 h of bacterial incubation on the skin, PL, PL-C, PL-DES and PL-(DES + C) film samples (2.5 × 2.5 cm²) were applied on the skin pieces, one piece of skin per sampling time for each sample and for controls. Additionally, a bacterial control (not contaminated) to which only PBS was added was used to verify the efficiency of the skin disinfection. All skin pieces were incubated for 45 min in the dark, to promote the photosensitizer binding to bacterial cells. Posteriorly, all samples and respective controls were irradiated using a light at 50 mW.cm⁻² for 180 min for *S. aureus* ATCC 6538 and 270 min for both MRSA strains divided by cycles of irradiation of 90 min each. For each cycle, a new sample of pullulan-based film was applied to the skin over the initial sample and moistened with 200 µL of PBS to maintain the skin humidity at surface. Dark controls were also performed alongside the aPDT samples. After specific time points (0, 90, 180 or 270 min) of irradiation, samples were collected and the bacteria were removed from each skin portion by sterile cotton wool swabs, 30 times each. The bacteria present in the cotton wool swabs were suspended in 1.0 mL of PBS, serially diluted in PBS, and each sample dilution was pour-plated using TSA as culture medium. The plates were incubated at 37 °C for 24 h and the CFU.mL⁻¹ was counted in all samples. Experiments were carried out in triplicated and repeated three times for each condition.

2.17. Statistical analysis

The results presented are expressed as mean ± standard deviation of at least three independent experiments with three different measurements. In the case of mechanical studies, at least 5 different specimens were used for each measurement. The statistical analysis of all data was done using a one-way ANOVA, with multiple comparisons. The levels of significance were set at probabilities of **p* < 0.02, ***p* < 0.002, ****p* < 0.0002 and *****p* < 0.0001 for moisture uptake assays, **p* < 0.01, ****p* < 0.0007 and *****p* < 0.0001 for mechanical assays, *p* < 0.01 and *p* < 0.002 for interfacial toughness and adhesive strength, respectively, and of *p* < 0.04 and **p* < 0.001, for the cytotoxicity experiments, all analyzed with Graphpad Prism 8.0.1 software (GraphPad Software, San Diego, CA, USA).

3. Results and discussion

This work focused on the development and characterization of pullulan (PL)-based films loaded with a DES-curcumin formulation, presenting improved mechanical, adhesive and antimicrobial photodynamic properties for application in aPDT of bacterial resistant skin infections. The DES composed of betaine (*N,N,N*-trimethylglycine) and levulinic acid (Bet:Lev), in a 1:1 M ratio, was selected due to the known acceptance of both components in skin care products [35,40].

The integrity of the pristine DES components in the formulation was confirmed by ^1H and ^{13}C NMR spectroscopy, as shown in [Supplementary Figs. 1a and 1b](#), respectively. The DES was used to tune the properties of the pullulan-based films, while allowing to enhance the solubility and photostability of the photosensitizer. Curcumin was solubilized in an aqueous solution of 50% (w/w) of Bet:Lev, herein used as a co-solvent, and whose concentration was selected according with optimization studies ([Supplementary Fig. 2](#)). The use of this solution allowed to achieve remarkable concentrations of $1.4 \times 10^4 \mu\text{M}$ and $2.6 \times 10^4 \mu\text{M}$ of curcumin in aqueous media at room and body's temperature, respectively. The solubility enhancement was accompanied by the extension of the curcumin's photostability (only 48–59% loss of the initial amount vs 100% loss in common solvent media like aqueous acetone in 60 min – cf. [Supplementary Fig. 3](#)). Furthermore, the aqueous Bet:Lev studied here does not require to be removed from the final formulations and can be advantageously used in the development of the delivery system.

Following this, pullulan adhesive films with $ca. 353 \pm 68 \mu\text{m}$ of thickness were prepared by solvent-casting of a 6% (w/v) pullulan solution containing the photosensitizer (20 μM) in the aqueous solution of Bet:Lev ([Fig. 1a](#)), resulting in films PL-(DES + C) containing $4.4 \mu\text{g}\cdot\text{cm}^{-2}$ of curcumin dose to be administered. Pullulan films loaded with curcumin solutions in aqueous acetone (PL-C) with a $4.4 \mu\text{g}\cdot\text{cm}^{-2}$ of curcumin dose were also studied. Additionally, pure pullulan films (PL) and films only with aqueous Bet:Lev (PL-DES) were prepared for comparison purposes. All obtained films were characterized in terms of their optical properties, structure, mechanical performance, adhesiveness to skin, cytotoxicity towards immortalized human epidermal keratinocytes (HaCaT cells) and antimicrobial activity against different *S. aureus*. The application of these adhesive films in the treatment of skin infections was also investigated on *ex vivo* skin samples to evaluate their ability to inactivate MRSA strains relevant in the clinical setting ([Fig. 1b](#)).

3.1. Optical, structural and thermal characterization

The visual aspect of the films, when typically applied on *ex vivo* skin,

are depicted in [Fig. 2a](#). All the prepared films are homogeneous and without insoluble particles. While PL and PL-DES based films are colorless and transparent, PL-C and PL-(DES + C) show a uniform yellow color, which is characteristic of the photosensitizer, but are still considerably transparent.

The optical properties of the films were also accessed by measuring their transmittances in the range of 200–700 nm ([Fig. 2b](#)). The spectrum of PL agrees with its visual aspect, indicating that the film is optically transparent, with transmittance values of 75–81% in the visible range (400–700 nm) and up to 75% in the ultraviolet range (200–400 nm), which are consistent with previously reported data [[22](#)]. The addition of Bet:Lev did not impact the film transparency, and, accordingly, the transmittance values in the visible range remained above 75% as for the pure PL films. Yet, the incorporation of curcumin slightly decreased the transparency of the films, namely PL-C to 50–80% and PL-(DES + C) to 48–76% in the visible range, due to the intense yellow color of the photosensitizer, which absorbs energy in the visible region (near 425 nm), as depicted in [Fig. 2b](#). However, the considerable preservation of transparency is particularly relevant to ensure the adequate irradiation of the photosensitizer essential for the antimicrobial action in the aPDT.

The FTIR-ATR spectrum of PL ([Fig. 2c](#)) shows the characteristic absorption bands of this polysaccharide at 3280 cm^{-1} , consistent with the O–H stretching vibration of the hydroxyl groups, and at 2918 and 2900 cm^{-1} corresponding to the C–H and CH_2 stretching vibrations, respectively [[22,41](#)]. The C–O–C stretching of the glycosidic bridges are observed in the region of 1176 to 940 cm^{-1} , whereas the typical α -glycosidic bond stretching appears at 850 cm^{-1} . The incorporation of curcumin solubilized in acetone in the biopolymer matrix does not lead to significant differences due to the low amount of the photosensitizer used in the film preparation. However, the loading of Bet:Lev into the pullulan film leads to the appearance of some characteristic bands of the DES, particularly at 1710 cm^{-1} related to the -COO- stretching vibration of both DES components [[42](#)]. However, when considering the spectra of the PL-DES and PL-(DES + C) films, interestingly, the most significant difference when compared with those of both PL and PL-C films is the

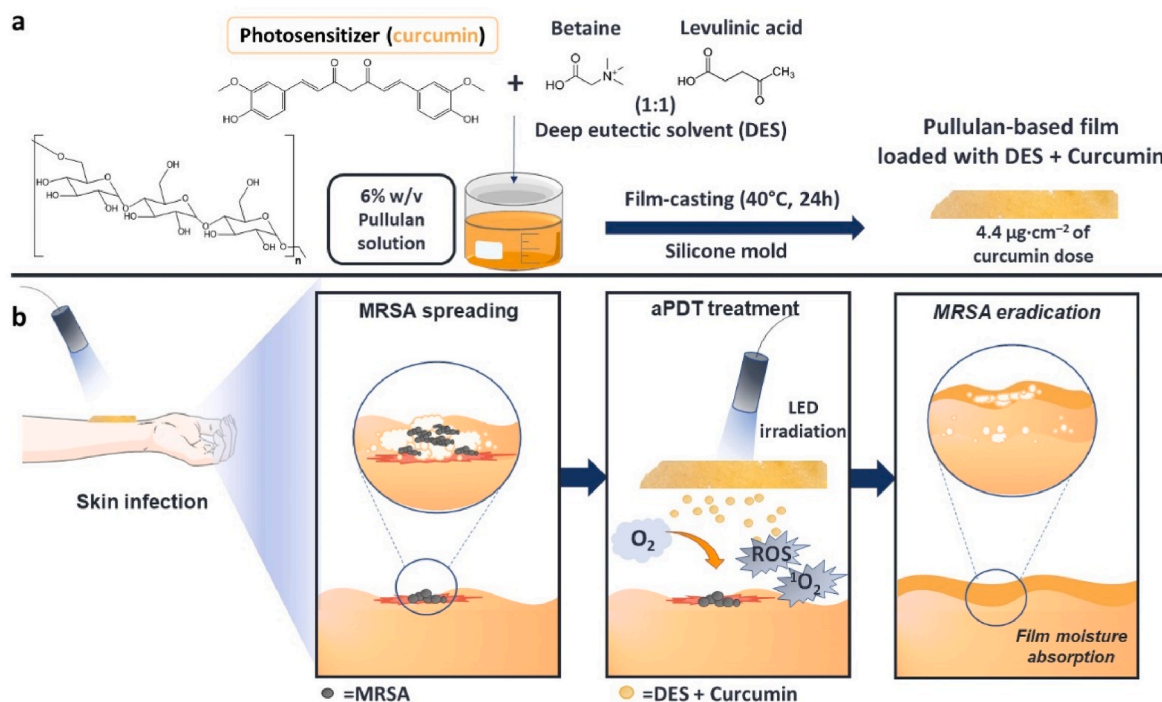


Fig. 1. Schematic illustration of the (a) preparation and (b) application of pullulan-based hydrogel films loaded with Bet:LevS comprising curcumin in the treatment of skin infections using the aPDT approach. Made using arm clipart from Servier Medical Art and adapted by the authors according with Servier under the CC-BY 3.0 License (at <https://smart.servier.com/>, accessed on June 15, 2022).

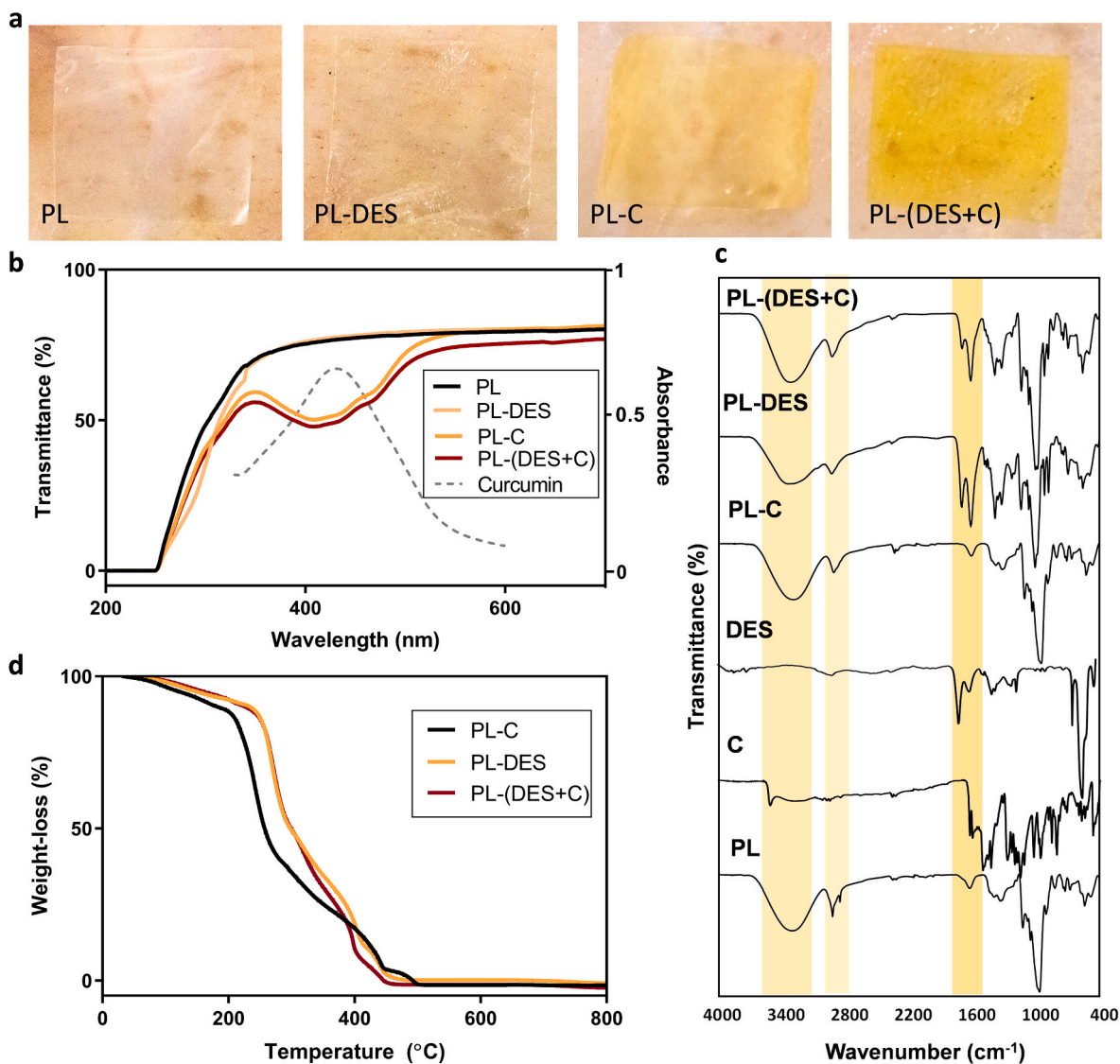


Fig. 2. (a) Visual appearance of the pullulan-based films (PL) loaded with Bet:Lev (PL-DES), comprising curcumin (PL-C) and with the DES and curcumin formulation (PL-(DES + C)) placed onto the ex-vivo porcine skin. (b) UV-vis spectra of the films (solid lines) and absorption profile of curcumin (dashed line). (c) FTIR-ATR spectra of all films and of the DES and curcumin used in the Bet:Lev formulations, presented for comparison purposes. (d) Thermograms of the studied pullulan systems with different compositions.

bending motion of the adsorbed water at 1621 cm^{-1} , which is particularly increased due to the high-water sensitivity of the pullulan films with the DES [42]. This could be related with the high water affinity of the DES and in part with the decrease in the strong intramolecular interactions between the polymeric chains, which are in part replaced by intermolecular hydrogen bonding between pullulan and Bet:Lev, as happens with the addition of plasticizers [43].

Thermogravimetric analysis (TGA) of the pullulan-based films was performed under a nitrogen atmosphere. The respective thermograms are provided in Fig. 2d. The thermal degradation profile of pullulan follows a single weight-loss step with initial and maximum decomposition temperatures of 273 and 400 °C, respectively, leaving a residue at 800 °C corresponding to about 20% of the initial mass. This single-step degradation profile can be associated with the degradation of the PL skeleton and is in accordance with previous findings [22]. The incorporation of Bet:Lev into pullulan films led to a slight decrease in the thermal stability in comparison to the pristine polysaccharide, decreasing the maximum decomposition temperatures to 253 °C for PL-DES and 241 °C for PL-(DES + C). This alteration can be attributed to the fact that the incorporation of Bet:Lev decreases the interactions

between the pullulan chains, thereby decreasing its stability. Such modifications have been also reported for the incorporation of these co-solvents in other biopolymer matrices, like nanocellulose [44]. Despite this decrease and the thermal degradation of curcumin observed at 171 °C (both in PL-C and PL-(DES + C)), these values are still above the adequate range for typical sterilization procedures, which take place around 120 °C for biomedical purposes [45].

3.2. Moisture uptake and mechanical performance

The moisture-uptake capacity of PL, PL-C, PL-DES and PL-(DES + C) was determined by submitting the films to different controlled atmosphere humidity conditions. For this, samples were kept at 54% of RH over 48 h, to understand their behavior in conditions close to those found when in contact with hydrated skin (Fig. 3a). and at 98% of RH to evaluate their moisture uptake in extreme moisture conditions, since in case of infections, exudates are commonly found [46] (Fig. 3b). The low moisture uptake values observed for the PL (7.2%) and PL-C (7.2%) films, at both humidity conditions after 48 h of exposure, confirmed the non-hygroscopic nature of pullulan. However, the addition of Bet:Lev to

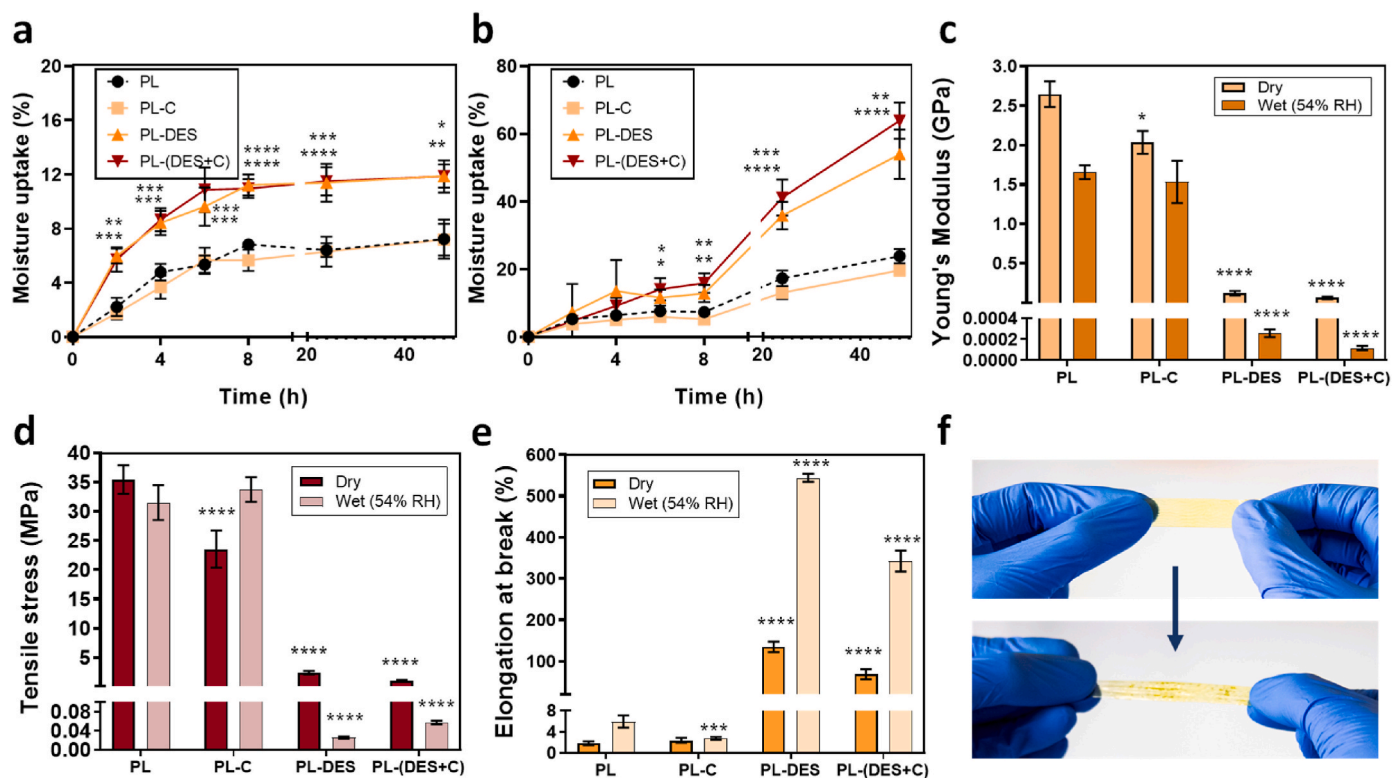


Fig. 3. Moisture-uptake capacity of PL, PL-C, PL-DES and PL-(DES + C) after being in a chamber with controlled humidity of (a) 54% RH and (b) 98% RH, for 48 h at room temperature. * $p < 0.02$, ** $p < 0.002$, *** $p < 0.0002$ and **** $p < 0.0001$, calculated through one-way ANOVA, in comparison to PL. (c) Young's modulus (GPa), (d) tensile stress (MPa) and (e) elongation at break (%) of the pullulan-based films in dry and wet (54% RH) conditions. The results are expressed as mean \pm SD. Levels of significance were set at probabilities of * $p < 0.01$, *** $p < 0.0007$ and **** $p < 0.0001$, calculated through one-way ANOVA and in comparison, to the PL system. (f) Graphical display of the extensibility of the PL-(DES + C) adhesive film in dry conditions.

the pullulan matrix considerably improved the moisture uptake capacity of the films, allowing a 2-fold increase in the humidity absorption at 54% RH (Fig. 3a) and 3-fold at 98% RH. Specifically, the moisture uptake of PL-DES and PL-(DES + C) films, reached 12.2% and 11.8% at 54% RH and 51.4% and 63.7% at 98% RH, respectively. This behavior is highly desired for the intended application, because after application, the films can absorb skin moisture (and exudates at the infection site), and maintain the hydration of the affected area. Moreover, the absorption of humidity will allow the film transition into a hydrogel with improved delivery of the photosensitizer and a better contact with the bacterial cells. Another important factor that can be affected by the moisture uptake enhancement by the incorporation of DES formulation is the mechanical performance of the studied films, which were evaluated by tensile tests. The Young's modulus, tensile stress and elongation at break were determined from the corresponding stress-strain curves, determined in dry (immediately after preparation) and in wet conditions (after a 24 h exposure to a 54% RH atmosphere, close to skin conditions) (Fig. 3c–e).

Dried PL films present high stiffness as confirmed by their easily breakable nature during handling, and by the high Young's modulus (2.7 GPa, Fig. 3c) and tensile stress (35.4 MPa, Fig. 3d), and low elongation at break (1.81%, Fig. 3e) values, which are in accordance with data previously reported for this polysaccharide [22,47]. The incorporation of curcumin (dissolved in acetone) into pullulan ($4.4 \mu\text{g}\cdot\text{cm}^{-2}$) has only a minimal impact on the mechanical performance, slightly decreasing the Young's modulus and the tensile stress to 2.0 GPa and 23.3 MPa, respectively, and increasing the elongation at break to 2.3%. Therefore, these films still present low plasticity and a brittle character, being difficult to adapt to the skin irregularities and to be used for topical applications. This behavior has been described when incorporating this photosensitizer into other biopolymer-based systems, such as

gelatin/chitosan [48] and carboxymethyl cellulose-based films [49]. After storage at 54% RH, PL films presented a slightly lower Young's modulus (1.6 GPa, Fig. 3c) and tensile stress (29.2 MPa, Fig. 3d) and higher elongation at break values (6.08%, Fig. 3e) than dried films. This behavior is associated with the incorporation of some water molecules in the biopolymer matrix that slightly weaken the interaction between the biopolymeric chains interaction, increasing their mobility.

The addition of the aqueous solution of Bet:Lev, on the other hand, has a remarkable effect on the mechanical performance of the prepared films, by promoting a significant decrease in the Young's modulus to around 100 MPa and in the tensile stress to 2.4 MPa, along with a noticeable increase in the elongation at break to 131.4%, in dry conditions. These results clearly disclose that Bet:Lev induces a strong plasticizer effect with a considerable influence on the mechanical properties of the resultant films, in agreement with other studies where different DES have been incorporated on polymeric materials [50,51]. Furthermore, when curcumin is added to the DES aqueous solution, its impact on the corresponding films (PL-(DES + C)) is verified by a decrease in the Young's modulus and the tensile stress, as well as elongation at break values, in comparison to the PL-DES films. For the PL-(DES + C) film, a Young's modulus of 60 MPa and a tensile stress of 1.04 MPa were observed, along with values of elongation at break of 68.2%. This can be attributed to the fact that the incorporation of the photosensitizer in the biopolymer matrix might create slight breaking points that allow an easier disruption of the PL-(DES + C) films than with the PL-DES [52]. Yet, it must be highlighted that the effect obtained with Bet:Lev in the PL-(DES + C), particularly on the improvement of extensibility of pullulan, is higher than that observed when using common plasticizers employed in the preparation of pullulan-based films, such as glycerol [22,43]. Thus, the results obtained with PL-(DES + C) surpass these values [53], particularly, at 54% RH, where a drastic increase in the

elongation at break to 546.5% for PL-DES and 338.2% for PL-(DES + C), a 4 to 5-fold increase, was verified. Concomitantly, a great decrease in the Young's modulus (2.6×10^{-4} GPa for PL-DES and 1.2×10^{-4} GPa for PL-(DES + C)) and tensile stress (2.5×10^{-2} MPa for PL-DES and 5.7×10^{-2} MPa for PL-(DES + C)) were also observed, (depicted in Fig. 3c–e).

Since skin infections can cause clinical manifestations, such as edema and skin deformation [53], the improvement in the film pliability is advantageous since it enables the system to better adapt and keep up with the skin elasticity. PL-(DES + C) system herein developed presents a high degree of stretchability when handled (even in dried conditions before skin application), as portrayed in Fig. 3f.

3.3. Adhesive properties

For photodynamic treatment purposes, adhesiveness might be particularly demanding, since the film loaded with the photosensitizer must be sustained at the infection site during the treatment period [54]. The adhesive capacity of the pullulan films prepared in this study (PL, PL-C, PL-DES and PL-(DES + C)) was evaluated through different mechanical tests, by measuring the interfacial toughness through peel tests (Fig. 4a) and the adhesive strength by lap-shear tests (Fig. 4b). Porcine skin was chosen as model tissue for this evaluation, due to its similarity to human skin [55]. After immediate application onto skin, both PL-DES and PL-(DES + C) maintain their solid film appearance and were able to establish tough adhesion with the porcine skin samples upon contact and after application of gentle pressure. However, after the application, the films with DES start to absorb the skin moisture, transiting into hydrogels, as portrayed in Fig. 4c and in Supplementary Video V1. These hydrogels, by contrast, exhibit remarkably higher interfacial toughness

values in comparison to the commercial system (Fig. 4b). This switchable character allows to enhance the interfacial toughness of the PL-DES film from values ranging from 47.3 to 124.6 J.m^{-2} , and even more notoriously from 44.27 to 252.78 J.m^{-2} for the PL-(DES + C) film. The interface toughness of PL-(DES + C) after switch into a hydrogel state presents a 2-fold increase in comparison to PL-DES and a 4-fold increase than that of the commercially available hydrocolloid Hydrocoll® (66.6 J.m^{-2}). This DES possess a high-water absorption capacity due to the hydrophilic nature of its components [56]; therefore, Bet:Lev might enhance the removal of interfacial water from the tissue surface, while also enabling the establishment of hydrogen bonding interactions between the biopolymer system with the skin epithelium [57]. In addition to the high adhesion capacity, these films highly withstand stress after adhesion. The adhesive strength of the films towards the porcine skin was found to be 2.1×10^3 kPa for PL-DES and 1.3×10^3 kPa for PL-(DES + C) (Fig. 4b). These values can be compared to other types of systems found in literature [25,58] and clearly highlight the positive effect of the incorporation of Bet:Lev into pullulan-based films in comparison to the pristine material [25].

3.4. Biocompatibility of DES formulations and pullulan-based systems

The cytotoxicity of curcumin, curcumin in aqueous solution with Bet:Lev and of the final adhesive system to be topically applied was initially determined on human keratinocytes (HaCaT cell line) (Fig. 5). Control groups were also studied cultivating them in the absence of the studied samples. Firstly, the influence of the aqueous Bet:Lev (50% (w/w)) on the overall toxicity of the formulations was appraised, after 24 h of exposure (Fig. 5). The aqueous Bet:Lev is non-cytotoxic to HaCaT cells in the studied concentration with cell viabilities above 80%; therefore, it will not significantly impact the cytotoxicity of the studied adhesive systems. Following this, the effect of curcumin on cell viability was accessed at the concentration included in the aqueous solution of 50% (w/w) of Bet:Lev during the previous experiments (20 μM).

Curcumin is non-cytotoxic in this concentration, with cell viabilities higher than 75%. This is expected since curcumin affects the non-cytotoxic cells viability in a dose-dependent manner. In fact, it was reported that at concentrations higher than 20 μM , curcumin effectively inhibited the proliferation and induced apoptosis of HaCaT cells with a rate as high as 34% [59,60]. Therefore, the concentration selected to be incorporated in the pullulan-based adhesive films is safe to be in contact with healthy skin cells. Finally, the cytotoxicity of the pullulan-based films containing curcumin (equivalent to a $4.4 \mu\text{g.cm}^{-2}$ dose) solubilized in aqueous Bet:Lev was evaluated. Our results reveal that both curcumin and aqueous Bet:Lev do not impact the overall cell viability of

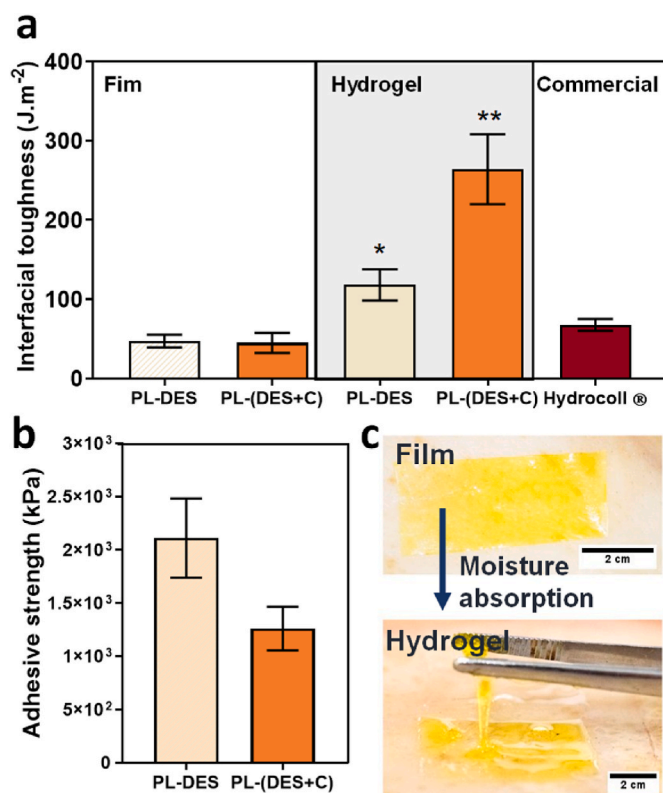


Fig. 4. Adhesion performance of PL-DES and PL-(DES + C) on porcine skin, determined by (a) interfacial toughness and (b) adhesive strength, respectively. * $p < 0.01$ and ** $p < 0.002$ increase in interfacial toughness in comparison to commercial adhesives (Hydrocoll®). (c) Visual appearance of the transition from solid to hydrogel of the PL-(DES + C) adhesive systems upon skin moisture absorption.

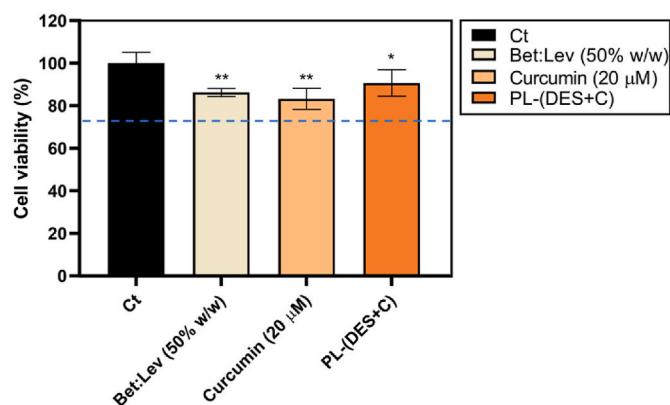


Fig. 5. Effect of Bet:Lev formulation (Bet:Lev 50% w/w) curcumin concentration (20 μM) in aqueous Bet:Lev and pullulan-based films (PL-(DES + C)) in the viability of HaCaT cells. Cytotoxicity profiles after 24 h of exposure vs control cells (Ct). Results are expressed as mean \pm SD of three independent experiments. * $p < 0.05$ and ** $p < 0.001$ cell viability compared to the control cells.

pullulan-based adhesive films (cell viability >80% obtained by direct exposure of the film to HaCaT cells). This could be expected since pullulan-based materials do not seem to present cytotoxicity towards this type of cell line [61], indicating their safeness for contact with healthy skin cells and being suitable for topical application.

3.5. *In vitro* antimicrobial action towards *S. aureus*

Skin and soft tissue infections can range from uncomplicated to invasive and life-threatening situations, of which *S. aureus* is a major contributor [62]. Therefore, the *S. aureus* ATCC 6538 strain was chosen to firstly address photodynamic antimicrobial action, given that it is used as reference in standard bactericidal tests. Since the effectiveness of aPDT can decrease with the sample complexity [63], it is particularly relevant to initially test controlled conditions. In this case, the aqueous solution of Bet:Lev comprising the photosensitizer was added directly to the bacterial suspension before testing it after incorporation in the pullulan film (Fig. 6a). Initially, the antimicrobial activity of the Bet:Lev aqueous solutions and of curcumin (20 μM) solubilized in these formulations (50% (w/w) of Bet:Lev in water) was assessed in the dark. Curcumin solution (20 μM) in an aqueous acetone (50% (w/w)) solution was also studied to infer about the curcumin's photodynamic activity in the absence of Bet:Lev. As indicated in Fig. 6b, without irradiation, none of the tested solutions displayed antimicrobial activity towards *S. aureus* ATCC 6538. Then, samples were incubated in the dark for 15 min and irradiated with a light dose of 50 $\text{mW}\cdot\text{cm}^{-2}$. In this case, it is possible to verify that both acetone and Bet:Lev do not affect the cell viability of the bacterium (Fig. 6c).

On the contrary, both curcumin aqueous solutions (20 μM) lead to successful bacterial reduction when irradiated. Thus, the bacterial reduction is owing to the photodynamic treatment. Specifically, curcumin in aqueous acetone leads to a 3.9 \log_{10} of inactivation ($p < 0.0001$) after 30 min of irradiation, decreasing to 4.2 \log_{10} of inactivation ($p <$

0.0001) after a 60 min with aPDT (Fig. 6c), while curcumin in aqueous Bet:Lev solution led to an abrupt inactivation of *S. aureus*, originated an 8.1 \log_{10} reduction ($p < 0.0001$) of the bacterium in only 30 min. The difference in the bactericidal activity between both samples can be attributed to the fact that not only curcumin is more prone to precipitate in the bacterial suspensions [64] when solubilized in an acetone solution but also curcumin dissolved in aqueous acetone completely degrades after 15 min (for further details - see Supplementary Fig. 3a). On the contrary, curcumin in aqueous Bet:Lev shows improved photostability (Supplementary Fig. 3b), enabling the photosensitizer to exert its effect for a longer period, being possible to fully inactivate *S. aureus* suspensions.

After the obtained promising results, the antimicrobial activity of the formulation incorporated in the adhesive film (4.4 $\mu\text{g}\cdot\text{cm}^{-2}$ of curcumin) was investigated. PL, PL-DES and PL-C were also tested for comparison purposes. Fig. 6d shows the photoinactivation profiles of *S. aureus* treated with all the pullulan-based films and with the control. Since the photosensitizer is loaded in the biopolymeric film, aPDT treatment was extended by an additional 30 min period to guarantee the complete release of curcumin into the media [65]. PL-C and PL-(DES + C) films exhibit a similar photoinactivation behavior in the first 15 min with a 3.2 \log_{10} reduction ($p < 0.0001$) of the viability of the bacterium. In contrast, in the PL-(DES + C), since the photosensitizer shows an enhanced photostability as previously stated, this is reflected in the complete photoinactivation of the bacteria after 60 min of the aPDT.

The mechanism of action of curcumin in aPDT, is typically associated with the generation of free radicals (type I mechanism) [66], as well as to the production of singlet oxygen (type II mechanism) [67]. To verify the main mechanism of action of curcumin in the PL-(DES + C), we used specific ROS scavengers (L-histidine for singlet oxygen and D-mannitol for free radicals) and studied their inhibitory effect (results presented in Supplementary Fig. 4). Given the decrease in curcumin's efficacy in the presence of L-histidine, it can be concluded that in the first 15 min the

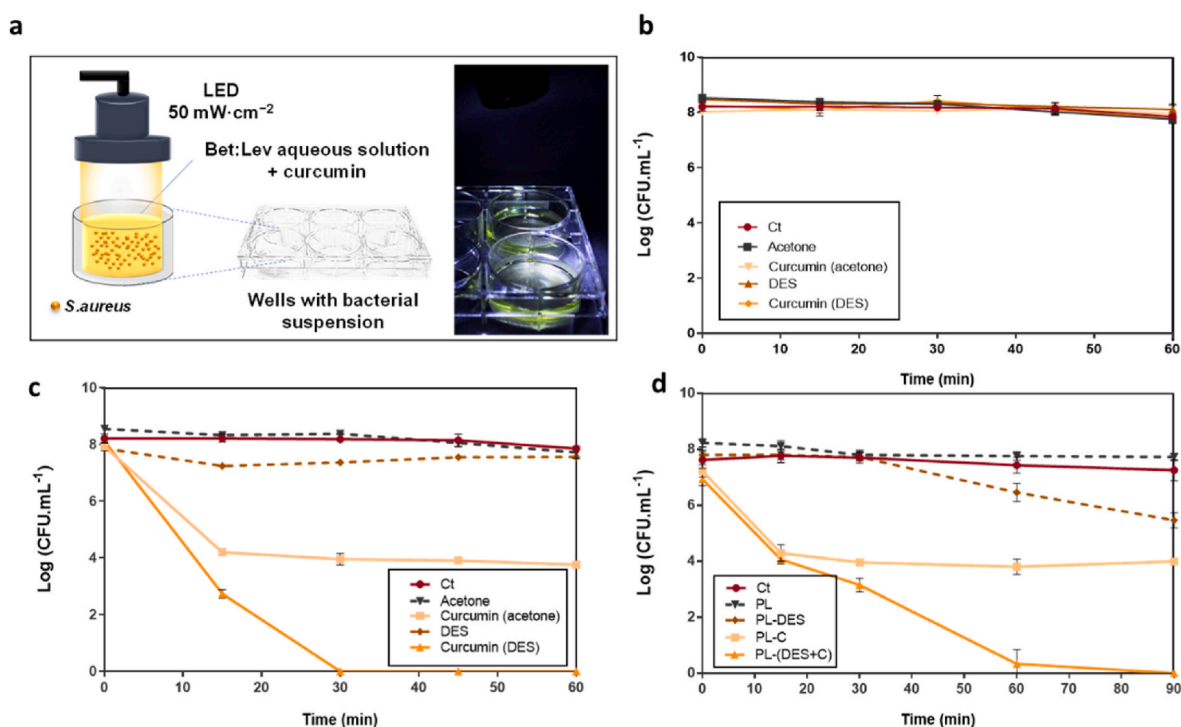


Fig. 6. (a) Schematic illustration of the *in vitro* aPDT assay process for the eradication of *S. aureus*. (b) Antimicrobial activity of each solution tested initially for dark controls. (c) Photoinactivation of *S. aureus* ATCC 6538 incubated with each sample and irradiated with LED at an irradiance of 50 $\text{mW}\cdot\text{cm}^{-2}$, using curcumin at 20 μM . (d) Photoinactivation profiles of *S. aureus* treated with pullulan-based films loaded with curcumin, with the DES, Bet:Lev and with Bet:Lev comprising curcumin. Light controls (Ct) represent the exposure of the bacteria to the same conditions in the absence of the photosensitizer. Results are expressed as mean \pm SD of three independent experiments with three replicates each.

production of singlet oxygen is more relevant for the photoinactivation efficacy. However, perhaps since oxygen is depleted from the media and the samples continue to be irradiated, the production of free radicals starts to have a similar contribution to photoinactivation of the bacterium. The obtained results indicate that unlike in some curcumin-based delivery systems, where the mechanism of action of curcumin is suggested to be solely of type II [67], in PL-(DES + C) both free radical and singlet oxygen take part in the process, fitting both type I and type II mechanisms of photoinactivation.

Given the high efficacy of the tested conditions and the bactericidal enhancement of the PL-(DES + C) system in comparison to the PL-C one, we further investigated their effect on infected skin samples.

3.6. Bacterial photoinactivation on an ex vivo skin model

To better evaluate the final effectiveness of the aPDT using the developed adhesive films against *S. aureus* ATCC 6538, the aPDT conditions were first adjusted in skin. Following this, the treatments on skin samples contaminated with MRSA DSM 25693 and with MRSA M98070, a clinically isolated strain that comprehend different colonization and toxin factors, were conducted. Aiming to resemble the conditions found

in *in vivo* skin infections, porcine skin samples were individually contaminated with each strain. The adhesive films were placed over the contaminated site and the photosensitizer was allowed to incubate. During the incubation period the adhesive absorbs skin moisture and switches into a hydrogel, as previously described. After this, the samples were irradiated with a light dose of $50 \text{ mW}\cdot\text{cm}^{-2}$ over 90 min. Owing to the skin complexity, photoinactivation is not as simple to attain as it is *in vitro* suspension. Therefore, attempting to achieve high inactivation rates, initially two cycles of 90 min irradiation each were performed, using a new adhesive in each cycle. Fig. 7a illustrates aPDT treatment cycle using the PL-(DES + C) adhesive films on infected skin for a better understanding.

The *ex vivo* experiments were first conducted for the same photosensitizer concentrations (topical application of $4.4 \mu\text{g}\cdot\text{cm}^{-2}$ of curcumin dose) and irradiance source ($50 \text{ mW}\cdot\text{cm}^{-2}$), tested in the previous assays but extending the dark incubation time from 15 to 45 min. This modification was considered since it has been already shown that a prolonged incubation period is required in the transition from *ex vivo* skin model as compared to the *in vitro* circumstances [63]. This update in the aPDT did not produce relevant alterations regarding the action of PL-C on *S. aureus* ATCC 6538 (Fig. 7b). Even after 2 cycles of aPDT, no

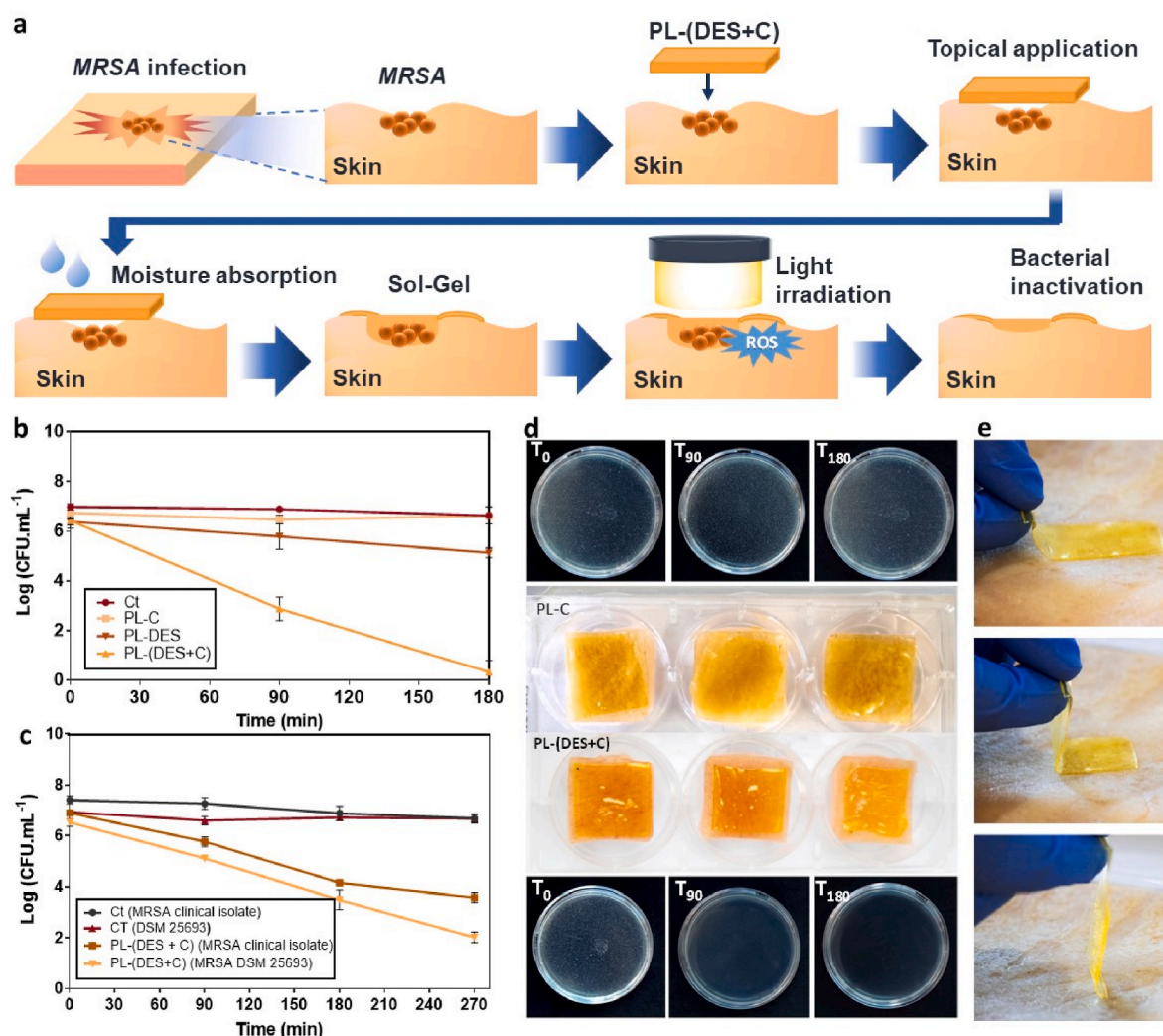


Fig. 7. (a) Graphic representation of an aPDT treatment cycle using the adhesive film PL-(DES + C). (b) Photoinactivation of *S. aureus* ATCC 6538 by pullulan-based films irradiated with LED at an irradiance of $50 \text{ mW}\cdot\text{cm}^{-2}$. (c) Photoinactivation of MRSA DSM 25693 and MRSA strain clinically isolated, treated with the adhesive film PL-(DES + C) (d) Visual appearance of the aPDT treatment with PL-C and PL-(DES + C) and its impact on skin samples contaminated with *S. aureus* ATCC 6538. Results are expressed as mean \pm SD of three independent treatments with three replicates each; and (e) photographs of the skin application and removal of PL-(DES + C) adhesives ($2.5 \times 5 \text{ cm}^2$).

inactivation of the bacterium is verified when applying PL-C, and the viability of the bacterium was not affected in the dark controls (data not shown). However, when the PL-(DES + C) adhesive was used, a 2.6 \log_{10} reduction ($p < 0.0001$) is observed over one cycle of the aPDT. Over two cycles of the aPDT it is possible to inactivate the bacterium down to the detection limit of the method (Fig. 7b). In addition, the PL-DES system shows only a slight impact in the photoinactivation, allowing 1.5 \log_{10} reduction ($p < 0.0001$). Based on these results, it is possible to conclude that the efficacy of PL-(DES + C) adhesive is not only due to the photodynamic treatment, but also to a synergistic effect between Bet:Lev and curcumin.

As shown in Fig. 7c, by observation of the respective agar plates used in the photodynamic experiments, the PL-C films do not exhibit any bacterial killing effect; thus, the continuous application of the PL-(DES + C) adhesives seems to be an effective strategy to treat *S. aureus* infections. Such fact prompted us to apply these adhesives in skin samples infected with MRSA strains, under the same conditions. Interestingly, these systems also show high photodynamic antimicrobial ability, enabling a similar inactivation profile for both MRSA strains over two cycles of photoinactivation (Fig. 7d). However, for these two bacterial strains an additional aPDT cycle was necessary. With this addition, it is possible to inactivate MRSA DSM 25693 ($>4.7 \log_{10}$) down to the detection limit of the method and to obtain a reduction of 3.3 \log_{10} ($p < 0.0001$) in the bacterial viability of the clinically isolated MRSA strain. The increase in the incubation period, where the PL-(DES + C) adhesive gradual switches from a solid film into a thick hydrogel, together with the high stability of the curcumin in this system, allows to deliver the photosensitizer in the infected area. As result, not only the adhesion of the photosensitizer to the bacteria is enhanced, but more importantly, the combined delivery of both Bet:Lev and the photosensitizer might improve their permeation into the bacterial cell membrane. Thus, a higher yield of ROS, both singlet oxygen and free radicals, is likely achieved upon the treatment. This contrasts with the reported reduced attachment and penetration of photosensitizers in *ex vivo* and *in vivo* conditions, which lead to a lower inactivation efficacy [68]. As herein verified, the antimicrobial activity is enhanced even in situations where agglomeration and biofilm formation can be foreseen, such as verified for the results of contaminations with both MRSA strains. MRSA strains obtained from chronic wounds seem to harbor more virulent genes compared to other strains and different abilities for biofilm formation [69]. Such a fact can justify the slight difference between the photoinactivation of *S. aureus* ATCC 6538 and of both MRSA strains after four cycles of the aPDT. Furthermore, by using the adhesive film with Bet:Lev and curcumin, it is achieved a higher killing efficacy than liquid porphyrinic formulations tested *ex vivo* on skin contaminated with similar MRSA strains [70]. The application of these liquid formulations usually implies the use of water-ethanol solutions, which are not only associated with the photobleaching of the photosensitizer, but also dry the *stratum corneum* impacting the efficacy of the aPDT in skin samples.

The systems herein developed are capable to overcome the drawbacks of liquid formulations without causing skin staining after application, particularly in the adhesive film form (as portrayed in Fig. 7e) and also after transition into the hydrogel. More importantly, these adhesives can be easily removed after the treatment (in hydrogel form) with water, due to the soluble character of all employed components, while being gentle to skin.

4. Conclusions

In this study, pullulan-based adhesive films loaded with Bet:Lev and curcumin formulations were developed. The selection and use of 50% (w/w) aqueous Bet:Lev allowed not only to solubilize curcumin in aqueous media, but also enabled to extend its photostability and the incorporation in an hydrophilic matrix like pullulan. The resultant pullulan-based films presented enhanced mechanical properties, namely higher moisture uptake capacity, extensibility and adhesive properties.

The developed adhesive films present a switchable character, being capable to absorb skin moisture, and thus passing from solid films to strong adhesive hydrogels with higher adhesiveness than commercial hydrogels (4-fold increase). These adhesives are capable to deliver the photosensitizer in specific skin areas, with no significant cytotoxicity associated (HaCaT cell viability $>80\%$). More importantly, the combination of these properties provides a higher therapeutic effect than the photosensitizer solubilized in common solvents such as acetone. This translates into a higher *in vitro* photodynamic antimicrobial action against *S. aureus* ATCC 6538 during the aPDT. PL-(DES + C) adhesive films allow to decrease the viability of multidrug-resistant bacteria, such as MRSA strains, below the detection limit of the method when tested in *ex vivo* skin sample models. These results are of high relevance since the PL-C films do not present antimicrobial activity in any of the *ex vivo* assays. Overall, the developed novel switchable adhesive films loaded with curcumin solutions in aqueous Bet:Lev proved to be effective systems to eradicate skin infections caused by drug-resistant strains.

Author contribution

Sónia N. Pedro: Conceptualization, Investigation, Methodology, Writing – original draft, Writing – review & editing. Bruno F. A. Valente: Investigation, Writing – review & editing. Carla Vilela: Methodology, Resources, Writing – review. Helena Oliveira: Methodology, Resources, Writing – review. Adelaide Almeida: Methodology, Resources, Writing – review. Mara G. Freire: Conceptualization, Methodology, Resources, Funding acquisition, Supervision, Writing – review. Armando J. D. Silvestre: Conceptualization, Methodology, Resources, Funding acquisition, Supervision, Writing – review. Carmen S. R. Freire: Conceptualization, Methodology, Project administration, Resources, Funding acquisition, Supervision, Writing – review

Declaration of competing interest

The authors declare that they have no known competing financial interests or personal relationships that could have appeared to influence the work reported in this paper.

Data availability

All data was included in the manuscript in the form of figures, graphics or tables

Acknowledgements

This work was developed within the scope of the project CICECO-Aveiro Institute of Materials, UIDB/50011/2020, UIDP/50011/2020 & LA/P/0006/2020, financed by national funds through the FCT/MEC (PIDDAC) and CESAM, UIDP/50017/2020, UIDB/50017/2020 & LA/P/0094/2020, financed by national funds through the FCT/MEC and when appropriate co-financed by FEDER under the PT2020 Partnership Agreement. FCT is also acknowledged for the doctoral grant (SFR H/BD/132584/2017) to S.N.P. and the research contracts under Scientific Employment Stimulus to H.O. (CEECIND/04050/2017), C.V. (CEECIND/00263/2018 and 2021.01571.CEECIND) and C.S.R.F. (CEECIND/00464/2017).

Appendix A. Supplementary data

Supplementary data to this article can be found online at <https://doi.org/10.1016/j.mtbio.2023.100733>.

References

- [1] C.J. Murray, K.S. Ikuta, F. Sharara, L. et al., Global burden of bacterial antimicrobial resistance in 2019: a systematic analysis, *Lancet* 399 (2022) 629–655, [https://doi.org/10.1016/S0140-6736\(21\)02724-0](https://doi.org/10.1016/S0140-6736(21)02724-0).
- [2] C. Llor, L. Bjerrum, Antimicrobial resistance: risk associated with antibiotic overuse and initiatives to reduce the problem, *Ther. Adv. Drug Saf.* 5 (2014) 229–241, <https://doi.org/10.1177/2042098614554919>.
- [3] M.Z. David, R.S. Daum, Community-associated methicillin-resistant *Staphylococcus aureus*: epidemiology and clinical consequences of an emerging epidemic, *Clin. Microbiol. Rev.* 23 (2010) 616–687, <https://doi.org/10.1128/CMR.00081-09>.
- [4] J. Cabral, A.G. R. Blue light disinfection in hospital infection control: advantages, drawbacks, and pitfalls, *Antibiotics* 8 (2019) 58, <https://doi.org/10.3390/antibiotics8020058>.
- [5] A. Tavares, S.R.S. Dias, C.M.B. Carvalho, M.A.F. Faustino, J.P.C. Tomé, M.G.P.M. S. Neves, A.C. Tomé, J.A.S. Cavaleiro, A. Cunha, N.C.M. Gomes, E. Alves, A. Almeida, Mechanisms of photodynamic inactivation of a Gram-negative recombinant bioluminescent bacterium by cationic porphyrins, *Photochem. Photobiol. Sci.* 10 (2011) 1659, <https://doi.org/10.1039/c1pp05097d>.
- [6] D. Alejandra, C. Méndez, E. Gutiérrez, E.J. Dionisio, M. Afonso, R. Buzalaf, R. C. Oliveira, M. Aparecida, A. Moreira, T. Cruvinel, Curcumin-mediated Antimicrobial Photodynamic Therapy reduces the viability and vitality of infected dentin caries microcosms, *Photodiagnosis Photodyn. Ther.* 24 (2018) 102–108, <https://doi.org/10.1016/j.pdpdt.2018.09.007>.
- [7] R.R. Kotha, D.L. Luthria, Curcumin: biological, pharmaceutical, nutraceutical, and analytical aspects, *Molecules* 24 (2019) 2930, <https://doi.org/10.3390/molecules24162930>.
- [8] S. Gnanasekar, G. Kasi, X. He, K. Zhang, L. Xu, E.-T. Kang, Recent advances in engineered polymeric materials for efficient photodynamic inactivation of bacterial pathogens, *Bioact. Mater.* 21 (2023) 157–174, <https://doi.org/10.1016/j.bioactmat.2022.08.011>.
- [9] S. Kim Haryanto, J.H. Kim, Kim J.O, S. Ku, H. Cho, D.H. Han, P. Huh, Fabrication of poly(ethylene oxide) hydrogels for wound dressing application using E-beam, *Macromol. Res.* 22 (2014) 131–138, <https://doi.org/10.1007/s13233-014-2023-z>.
- [10] S. Glass, T. Rüdiger, J. Griebel, B. Abel, A. Schulze, Uptake and release of photosensitizers in a hydrogel for applications in photodynamic therapy: the impact of structural parameters on intrapolymer transport dynamics, *RSC Adv.* 8 (2018) 41624–41632, <https://doi.org/10.1039/C8RA08093C>.
- [11] C.-C. Feng, W.-F. Lu, Y.-C. Liu, T.-H. Liu, Y.-C. Chen, H.-W. Chien, Y. Wei, H.-W. Chang, J. Yu, A hemostatic keratin/alginate hydrogel scaffold with methylene blue mediated antimicrobial photodynamic therapy, *J. Mater. Chem. B* 10 (2022) 4878–4888, <https://doi.org/10.1039/D2TB00898J>.
- [12] C.-P. Chen, C.-M. Hsieh, T. Tsai, J.-C. Yang, C.-T. Chen, Optimization and evaluation of a chitosan/hydroxypropyl methylcellulose hydrogel containing toluidine blue O for antimicrobial photodynamic inactivation, *Int. J. Mol. Sci.* 16 (2015) 20859–20872, <https://doi.org/10.3390/ijms160920859>.
- [13] M. Frade, S. de Annunzio, G. Calixto, F. Victorelli, M. Chorilli, C. Fontana, Assessment of chitosan-based hydrogel and photodynamic inactivation against propionibacterium acnes, *Molecules* 23 (2018) 473, <https://doi.org/10.3390/molecules23020473>.
- [14] S. Hu, X. Pei, L. Duan, Z. Zhu, Y. Liu, J. Chen, T. Chen, P. Ji, Q. Wan, J. Wang, A mussel-inspired film for adhesion to wet buccal tissue and efficient buccal drug delivery, *Nat. Commun.* 12 (2021), <https://doi.org/10.1038/s41467-021-21989-5>.
- [15] A.F. Borges, C. Silva, J.F.J. Coelho, S. Simões, Oral films: current status and future perspectives: I-Galenical development and quality attributes, *J. Contr. Release* 206 (2015) 1–19, <https://doi.org/10.1016/j.jconrel.2015.03.006>.
- [16] P. Kord Forooshani, B.P. Lee, Recent approaches in designing bioadhesive materials inspired by mussel adhesive protein, *J. Polym. Sci. A. Polym. Chem.* 55 (2017) 9–33, <https://doi.org/10.1002/pola.28368>.
- [17] T. Huang, Z. Zhou, Q. Li, X. Tang, X. Chen, Y. Ge, J. Ling, Light-triggered adhesive silk-based film for effective photodynamic antibacterial therapy and rapid hemostasis, *Front. Bioeng. Biotechnol.* 9 (2022), <https://doi.org/10.3389/fbioe.2021.820434>.
- [18] C. Mao, Y. Xiang, X. Liu, Z. Cui, X. Yang, Z. Li, S. Zhu, Y. Zheng, K.W.K. Yeung, S. Wu, Repeatable photodynamic therapy with triggered signaling pathways of fibroblast cell proliferation and differentiation to promote bacteria-accompanied wound healing, *ACS Nano* 12 (2018) 1747–1759, <https://doi.org/10.1021/acsnano.7b08500>.
- [19] X. Lei, L. Qiu, M. Lan, X. Du, S. Zhou, P. Cui, R. Zheng, P. Jiang, J. Wang, J. Xia, Antibacterial photodynamic peptides for staphylococcal skin infection, *Biomater. Sci.* 8 (2020) 6695–6702, <https://doi.org/10.1039/DOBM01467B>.
- [20] I.M. Garnica-Palafox, F.M. Sánchez-Arévalo, Influence of natural and synthetic crosslinking reagents on the structural and mechanical properties of chitosan-based hybrid hydrogels, *Carbohydr. Polym.* 151 (2016) 1073–1081, <https://doi.org/10.1016/j.carbpol.2016.06.036>.
- [21] X. Chen, T. Taguchi, Enhanced skin adhesive property of hydrophobically modified poly(vinyl alcohol) films, *ACS Omega* 5 (2020) 1519–1527, <https://doi.org/10.1021/acsomega.9b03305>.
- [22] N.H.C.S. Silva, C. Vilela, A. Almeida, I.M. Marrucho, C.S.R. Freire, Pullulan-based nanocomposite films for functional food packaging: exploiting lysozyme nanofibers as antibacterial and antioxidant reinforcing additives, *Food Hydrocolloids* 77 (2018) 921–930, <https://doi.org/10.1016/j.foodhyd.2017.11.039>.
- [23] M.B. Coltell, S. Danti, K. de Clerk, A. Lazzeri, P. Morganti, Pullulan for advanced sustainable body- and skin-contact applications, *J. Funct. Biomater.* 11 (2020), <https://doi.org/10.3390/jfb11010020>.
- [24] K.-C. Cheng, A. Demirci, J.M. Catchmark, Pullulan: biosynthesis, production, and applications, *Appl. Microbiol. Biotechnol.* 92 (2011) 29–44, <https://doi.org/10.1007/s00253-011-3477-y>.
- [25] V.S. Priya, K. Iyappan, V.S. Gayahtri, S. William, L. Suguna, Influence of pullulan hydrogel on sutureless wound healing in rats, *Wound Medicine* 14 (2016) 1–5, <https://doi.org/10.1016/j.wndm.2016.05.003>.
- [26] N.M.N. Le, B. Le-Vinh, J.D. Friedl, A. Jalil, G. Kali, A. Bernkop-Schnürch, Polyaminated pullulan, a new biodegradable and cationic pullulan derivative for mucosal drug delivery, *Carbohydr. Polym.* 282 (2022), <https://doi.org/10.1016/j.carbpol.2022.119143>.
- [27] A.I. Riku Kawasaki, Reo Ohdake, Keita Yamana, Takuro Eto, Kouta Sugikawa, Photodynamic therapy using self-assembled nanogels comprising chlorin e6-bearing pullulan, *J. Mater. Chem. B* 9 (2021) 6357–6363.
- [28] B. Bae, K. Na, Self-quenching polysaccharide-based nanogels of pullulan/folate-photosensitizer conjugates for photodynamic therapy, *Biomaterials* 31 (2010) 6325–6335, <https://doi.org/10.1016/j.biomaterials.2010.04.030>.
- [29] B. chan Bae, K. Na, Self-quenching polysaccharide-based nanogels of pullulan/folate-photosensitizer conjugates for photodynamic therapy, *Biomaterials* 31 (2010) 6325–6335, <https://doi.org/10.1016/j.biomaterials.2010.04.030>.
- [30] S. Lee, K. Na, Oleic acid conjugated polymeric photosensitizer for metastatic cancer targeting in photodynamic therapy, *Biomater. Res.* 24 (2020), <https://doi.org/10.1186/s40824-019-0177-7>.
- [31] M.A.R. Martins, S.P. Pinho, J.A.P. Coutinho, Insights into the nature of eutectic and deep eutectic mixtures, *J. Solut. Chem.* (2018) 1–21, <https://doi.org/10.1007/s10953-018-0793-1>.
- [32] A.P. Abbott, E.I. Ahmed, K. Prasad, I.B. Qader, K.S. Ryder, Liquid pharmaceuticals formulation by eutectic formation, *Fluid Phase Equil.* 448 (2017) 2–8, <https://doi.org/10.1016/j.fluid.2017.05.009>.
- [33] S.N. Pedro, A.T.P.C. Gomes, P. Oskoei, H. Oliveira, A. Almeida, M.G. Freire, A.J. D. Silvestre, C.S.R. Freire, Boosting antibiotics performance by new formulations with deep eutectic solvents, *Int. J. Pharm.* 616 (2022), 121566, <https://doi.org/10.1016/j.ijpharm.2022.121566>.
- [34] S.N. Pedro, M.S.M. Mendes, B.M. Neves, I.F. Almeida, P. Costa, I. Correia-Sá, C. Vilela, M.G. Freire, A.J.D. Silvestre, C.S.R. Freire, Deep eutectic solvent formulations and alginate-based hydrogels as a new partnership for the transdermal administration of anti-inflammatory drugs, *Pharmaceutics* 14 (2022) 827, <https://doi.org/10.3390/pharmaceutics14040827>.
- [35] Q. Garrett, N. Khandekar, S. Shih, J.L. Flanagan, P. Simmons, J. Vehige, M.D. P. Willcox, Betaine stabilizes cell volume and protects against apoptosis in human corneal epithelial cells under hyperosmotic stress, *Exp. Eye Res.* 108 (2013) 33–41, <https://doi.org/10.1016/j.exer.2012.12.001>.
- [36] P.B. Sánchez, B. González, J. Salgado, J. José Parajó, Á. Domínguez, Physical properties of seven deep eutectic solvents based on L-proline or betaine, *J. Chem. Thermodyn.* 131 (2019) 517–523, <https://doi.org/10.1016/j.jct.2018.12.017>.
- [37] K.C. Zimmerman, T. Gilat Schmidt, J. Beck, M. Fedkin, S. Lvov, al., L. Qi Dong, B. Niu, H. Jian Liao, The Control of Humidity by Saturated Salt Solutions., n.d.
- [38] I. Baptista, R.P. Queirós, A. Cunha, J.A. Saraiva, S.M. Rocha, A. Almeida, Inactivation of enterotoxic and non-enterotoxic *Staphylococcus aureus* strains by high pressure treatments and evaluation of its impact on virulence factors, *Food Control* 57 (2015) 252–257, <https://doi.org/10.1016/j.foodcont.2015.04.022>.
- [39] L. Costa, M.A.F. Faustino, J.P.C. Tomé, M.G.P.M.S. Neves, A.C. Tomé, J.A. S. Cavaleiro, A. Cunha, A. Almeida, Involvement of type I and type II mechanisms on the photoinactivation of non-enveloped DNA and RNA bacteriophages, *J. Photochem. Photobiol., B* 120 (2013) 10–16, <https://doi.org/10.1016/j.jphotobiol.2013.01.005>.
- [40] S. Papageorgiou, A. Varvaresou, E. Tsihrivas, C. Demetzos, New alternatives to cosmetics preservation, *J. Cosmet. Sci.* 61 (2010) 107–123.
- [41] S.C.M. Fernandes, P. Sadocco, J. Causio, A.J.D. Silvestre, I. Mondragon, C.S. R. Freire, Antimicrobial pullulan derivative prepared by grafting with 3-aminopyrrolmethoxysilane: characterization and ability to form transparent films, *Food Hydrocolloids* 35 (2014) 247–252, <https://doi.org/10.1016/j.foodhyd.2013.05.014>.
- [42] G. Li, Q. Xie, Q. Liu, J. Liu, C. Wan, D. Liang, H. Zhang, Separation of phenolic compounds from oil mixtures by betaine-based deep eutectic solvents, *Asia-Pac. J. Chem. Eng.* 15 (2020) 1–10, <https://doi.org/10.1002/apj.2515>.
- [43] P.R. Vuddanda, M. Montenegro-Nicolini, J.O. Morales, S. Velaga, Effect of plasticizers on the physico-mechanical properties of pullulan based pharmaceutical oral films, *Eur. J. Pharmaceut. Sci.* 96 (2017) 290–298, <https://doi.org/10.1016/j.ejps.2016.09.011>.
- [44] J.G. Lynam, N. Kumar, M.J. Wong, Deep eutectic solvents' ability to solubilize lignin, cellulose, and hemicellulose; thermal stability; and density, *Bioresour. Technol.* 238 (2017) 684–689, <https://doi.org/10.1016/j.biortech.2017.04.079>.
- [45] D. Rafael, F. Andrade, F. Martinez-Trucharte, J. Basas, J. Seras-Franzoso, M. Palau, X. Gomis, M. Pérez-Burgos, A. Blanco, A. López-Fernández, R. Vélez, I. Abasolo, M. Aguirre, J. Gavalda, S. Schwartz, Sterilization procedure for temperature-sensitive hydrogels loaded with silver nanoparticles for clinical applications, *Nanomaterials* 9 (2019) 380, <https://doi.org/10.3390/nano9030380>.
- [46] E. Bouza, F.G. De Rosa, A. Guzek, T. Dirschka, G. Pellacani, Multidisciplinary panel opinion on the management of bacterial skin infections, *J. EADV Clinical Practice* 1 (2022) 165–175, <https://doi.org/10.1002/jvc2.43>.
- [47] I.A. de Lima, S.P. Pomin, O.A. Cavalcanti, Development and characterization of pullulan-polymethacrylate free films as potential material for enteric drug release, *Braz. J. Pharm. Sci.* 53 (2017) 1–9, <https://doi.org/10.1590/s2175-97902017000300002>.

- [48] F. Packaging, Gelatin/chitosan films incorporated with curcumin based on photodynamic inactivation Technology for antibacterial food packaging, *Polymers* 14 (2022) 1600, <https://doi.org/10.3390/polym14081600>.
- [49] S. Roy, J. Rhim, Carboxymethyl cellulose-based antioxidant and antimicrobial active packaging film incorporated with curcumin and zinc oxide, *Int. J. Biol. Macromol.* 148 (2020) 666–676, <https://doi.org/10.1016/j.ijbiomac.2020.01.204>.
- [50] C. Gao, E. Pollet, L. Averous, Properties of glycerol-plasticized alginate films obtained by thermo-mechanical mixing, *Food Hydrocolloids* 63 (2017) 414–420, <https://doi.org/10.1016/j.foodhyd.2016.09.023>.
- [51] M.P. Sokolova, M.A. Smirnov, A.A. Samarov, N.v. Bobrova, V.K. Vorobiov, E. N. Popova, E. Filippova, P. Geydt, E. Lahderanta, A.M. Toikka, Plasticizing of chitosan films with deep eutectic mixture of malonic acid and choline chloride, *Carbohydr. Polym.* 197 (2018) 548–557, <https://doi.org/10.1016/j.carbpol.2018.06.037>.
- [52] P.L. Implant, C. Matrices, D. Arbeiter, T. Reske, M. Teske, D. Bajer, V. Senz, K. Schmitz, N. Grabow, S. Oschatz, Influence of drug incorporation on the physico-chemical properties of poly(L-lactide) implant coating matrices—a systematic study, *Polymers* 13 (2021) 292, <https://doi.org/10.3390/polym13020292>.
- [53] V. Ki, C. Rostein, Bacterial skin and soft tissue infections in adults : a review of their epidemiology, pathogenesis , diagnosis , treatment and site of care, *Can. J. Infect Dis. Med. Microbiol.* 19 (2008) 173–184.
- [54] C. Spagnul, L.C. Turner, W. Boyle, Immobilized Photosensitisers for antimicrobial applications, *J. Photochem. Photobiol., B* 150 (2015) 11–30, <https://doi.org/10.1016/j.jphotobiol.2015.04.021>.
- [55] J. Li, A.D. Celiz, Q. Yang, I. Wamala, W. Whyte, B.R. Seo, N. v Vasilyev, J. J. Vlassak, Z. Suo, D.J. Mooney, Tough adhesives for diverse wet surfaces, *Science* 357 (1979) 378–381, 2017.
- [56] Y. Chen, D. Yu, W. Chen, L. Fu, T. Mu, Water absorption by deep eutectic solvents, *Phys. Chem. Chem. Phys.* 21 (2019) 2601–2610, <https://doi.org/10.1039/c8cp07383j>.
- [57] S. Singla, G. Amarpuri, N. Dhoptkar, T.A. Blackledge, A. Dhinojwala, Hygroscopic compounds in spider aggregate glue remove interfacial water to maintain adhesion in humid conditions, *Nat. Commun.* 9 (2018) 1890, <https://doi.org/10.1038/s41467-018-04263-z>.
- [58] J. Qu, X. Zhao, Y. Liang, T. Zhang, P.X. Ma, B. Guo, Antibacterial adhesive injectable hydrogels with rapid self-healing, extensibility and compressibility as wound dressing for joints skin wound healing, *Biomaterials* 183 (2018) 185–199, <https://doi.org/10.1016/j.biomaterials.2018.08.044>.
- [59] W. Song, Y. Ren, L. Liu, Y. Zhao, Q. Li, H. Yang, Curcumin induced the cell death of immortalized human keratinocytes (HaCaT) through caspaseindependent and caspase-dependent pathways, *Food Funct.* 12 (2021) 8669–8680, <https://doi.org/10.1039/d1fo01560e>.
- [60] Y. Zhao, J. Sun, W. Dou, J. Hu, Curcumin inhibits proliferation of interleukin-22-treated HaCaT cells, *Int. J. Clin. Exp. Med.* 8 (2015) 9580–9584.
- [61] D.F.S. Fonseca, P.C. Costa, I.F. Almeida, P. Dias-Pereira, I. Correia-Sá, V. Bastos, H. Oliveira, M. Duarte-Araújo, M. Morato, C. Vilela, A.J.D. Silvestre, C.S.R. Freire, Pullulan microneedle patches for the efficient transdermal administration of insulin envisioning diabetes treatment, *Carbohydr. Polym.* 241 (2020), 116314, <https://doi.org/10.1016/j.carbpol.2020.116314>.
- [62] S.Y.C. Tong, J.S. Davis, E. Eichenberger, T.L. Holland, V.G. Fowler, Staphylococcus aureus infections: epidemiology, pathophysiology, clinical manifestations, and management, *Clin. Microbiol. Rev.* 28 (2015) 603–661, <https://doi.org/10.1128/CMR.00134-14>.
- [63] T.M. Branco, N.C. Valério, V.I.R. Jesus, C.J. Dias, M.G.P.M.S. Neves, M.A. F. Faustino, A. Almeida, Single and combined effects of photodynamic therapy and antibiotics to inactivate Staphylococcus aureus on skin, *Photodiagnosis Photodyn. Ther.* 21 (2018) 285–293, <https://doi.org/10.1016/j.pdpdt.2018.01.001>.
- [64] O. Naksuriya, M.J. van Steenberg, J.S. Torano, S. Okonogi, W.E. Hennink, A kinetic degradation study of curcumin in its free form and loaded in polymeric micelles, *AAPS J.* 18 (2016) 777–787, <https://doi.org/10.1208/s12248-015-9863-0>.
- [65] K.A.D.F. Castro, N.M.M. Moura, F. Figueira, R.I. Ferreira, M.M.Q. Simões, J.A. S. Cavaleiro, M.A.F. Faustino, A.J.D. Silvestre, C.S.R. Freire, J.P.C. Tomé, S. Nakagaki, A. Almeida, M.G.P.M.S. Neves, New materials based on cationic porphyrins conjugated to chitosan or titanium dioxide: synthesis, characterization and antimicrobial efficacy, *Int. J. Mol. Sci.* 20 (2019) 2522, <https://doi.org/10.3390/ijms20102522>.
- [66] T.A. Dahl, W.M. McGowan, M.A. Shand, V.S. Srinivasan, Photokilling of bacteria by the natural dye curcumin, *Arch. Microbiol.* 151 (1989) 183–185, <https://doi.org/10.1007/BF00414437>.
- [67] L. Chen, Z. Song, X. Zhi, B. Du, Photoinduced antimicrobial activity of curcumin-containing coatings: molecular interaction, stability and potential application in food decontamination, *ACS Omega* 5 (2020) 31044–31054, <https://doi.org/10.1021/acsomega.0c04065>.
- [68] C.R. Fontana, A.D. Abernethy, S. Som, K. Ruggiero, S. Doucette, R.C. Marcantonio, C.I. Boussios, R. Kent, J.M. Goodson, A.C.R. Tanner, N.S. Soukos, The antibacterial effect of photodynamic therapy in dental plaque-derived biofilms, *J. Periodontol. Res.* 44 (2009) 751–759, <https://doi.org/10.1111/j.1600-0765.2008.01187.x>.
- [69] A. Budzyńska, K. Skowron, A. Kaczmarek, M. Wietlicka-Piszcz, E. Gospodarek-Komkowska, Virulence factor genes and antimicrobial susceptibility of Staphylococcus aureus strains isolated from blood and chronic wounds, *Toxins* 13 (2021) 491, <https://doi.org/10.3390/toxins13070491>.
- [70] T. Maisch, C. Bosl, R.M. Szeimies, B. Love, C. Abels, Determination of the antibacterial efficacy of a new porphyrin-based photosensitizer against MRSA ex vivo, *Photochem. Photobiol. Sci.* 6 (2007) 545–551, <https://doi.org/10.1039/b614770d>.